Review

Paleomagnetic-Geodynamic Mapping of the Transition Zone from Ocean to the Continent: A Review

Lev V. Eppelbaum [1,2,*] and **Youri I. Katz [3]**

1   Department of Geophysics, Faculty of Exact Sciences, Tel Aviv University, Ramat Aviv, Tel Aviv 6997801, Israel
2   Azerbaijan State Oil and Industry University, 20 Azadlig Ave., Baku AZ1010, Azerbaijan
3   Steinhardt Museum of Natural History & National Research Center, Faculty of Life Sciences,
    Tel Aviv University, Ramat Aviv, Tel Aviv 6997801, Israel; kiyour@mail.ru
*   Correspondence: levap@tauex.tau.ac.il

Abstract: The easternmost Mediterranean is a distinct transition zone from the ocean to the continent located at the junction between the largest Earth's lithospheric segments: Eurasian and African. The methodology of paleomagnetic mapping of such transition zones is based on integrating the mapping techniques for both continental and oceanic platforms: paleomagnetic reconstructions, results of radiometric dating of magnetized rocks, tectonic-structural reconstructions, biogeography, and utilization of the results of various geophysical surveys. The geodynamic-paleomagnetic mapping makes it possible to reveal the multilevel structural heterogeneity and display complex elements of the geodynamics of different ages inherent in this transition zone. The region of northern Israel is the most complex area in the easternmost Mediterranean. For the combined paleomagnetic mapping, well-studied paleomagnetically and radiometrically areas were selected: (1) the Carmel area, (2) the Atlit area (internal part of the Carmel area), (3) the Sea of Galilee with the adjoining zones (primarily, the Kinnarot Valley), and (4) the area of the Hula Basin with adjacent areas of the Golan Plateau, Hermon Mt., and Galilea uplift. The constructed paleomagnetic profiles for the Carmel area (on the top of the accumulative surface of the Lower Cretaceous traps) and the Kinnarot Valley—Sea of Galilee—Hula Basin, evidently indicate the complex history of the paleogeodynamic evolution of the region. These studies demonstrate the effectiveness of paleomagnetic mapping integrated with paleomagnetic profiles crossing these geologically complex areas.

Keywords: paleomagnetic mapping; paleomagnetic profiling; radiometric dating; tectonic-structural interpretation; integrated study

1. Introduction

The easternmost Mediterranean is a transition zone between the large tectonic-geodynamic structures of the Earth: Eurasian and African [1–5]. Unique structural features characterize the area that simultaneously expresses the elements of the tectonic collision associated with the evolution of the Tethys Ocean [6–8] and the initial spreading of the Red Sea rift system [9]. In the Cenozoic, four lithospheric plates intruded into the area: Nubian, Arabian, Aegean-Anatolian, and Sinai [10].

This tectonic-geodynamic setting is of extreme complexity and variegation of the developed tectonic elements and the rock complexes of the Earth's crust. The mentioned geological features form a very bizarre intersection, which combines heterogeneous continental and oceanic crust blocks, ophiolite belts, traps, folded island-arc, and terrane complexes, and the complex zones of strike-slip, thrusts, and underthrust faults [11–16].

The widespread development of the magmatic sequences of different ages and origins stimulated the employment of magnetic investigations in the region under study (e.g., [17–23]). Therefore, paleomagnetic methods are vital in considering the presence of a variety of arbitrary magnetized rocks. At the same time, the importance of paleomagnetic studies goes beyond just explaining the magnetic anomalies. Paleomagnetic data have

successfully recommended itself for deciphering the structure of the intricate targets from the subsurface up to the large depths in the continents and oceans [24–28].

Paleomagnetic methods were applied partially in the transition zones from ocean to continent [29]. However, their initial application in the easternmost Mediterranean region was triggered by the work of Ben-Avraham et al. [30]. The previous experience of our studies in this region [16,18,31–33] indicates that paleomagnetic studies are effective tools for analyzing the geodynamic-tectonic features of the easternmost Mediterranean.

The use of paleomagnetic-radiometric mapping (based on the integrated use of magnetostratigraphic divisions of different orders and corresponding radiometric data) in this region began with the research of Eppelbaum et al. [18,19]. This combined mapping can be applied primarily in areas with comprehensive paleomagnetic study accompanied by detailed radiometric dating. Besides this, the mentioned mapping demands knowledge of tectonic-structural reconstructions, drilling results, and different geophysical data analyses. We have significantly expanded the techniques and methods of the paleomagnetic mapping in the Easternmost Mediterranean, combining it with the regional gravity, magnetic and seismic data, and the structural analysis of sedimentary formations and crustal blocks that are discussed below.

2. Tectono-Paleomagnetic Mapping and Its Role in Geological-Geophysical Integration

Paleomagnetic research is widely accepted as a powerful independent tool for geodynamic and tectonic analysis, studying in-depth features, searching for economic minerals, and archaeogeophysical analysis (e.g., [24,26,28]). In principle, the geological-geophysical conclusions reached from paleomagnetic data analysis cannot be obtained using other geophysical or geological methods [22,34]. Regional and local magnetostratigraphic charts are widely applied to unify the stratigraphic schemes and correlate the numerous local subdivisions. Paleomagnetic mapping (zonation) can be realized in well-studied areas with detailed paleomagnetic measurements, radiometric dating, and structural-tectonic examination. Paleomagnetic mapping enables to "jump" from the single measurements to some areal reconstructions that increase the paleomagnetic method's effectiveness. At the same time, integration of paleomagnetic data with the set of geophysical-geological approaches often strongly increases the reliability and the significance of the combined research.

The first paleomagnetic stratigraphic studies in sedimentary rocks are associated with investigations by Irving and Runcorn [35]. The authors detected normal and reversed magnetic polarities in the Proterozoic Torridonian Sandstones and rocks from Scotland's Devonian and Triassic ages. For the Torridonian Sandstones, an attempt was made to correlate the observed polarity zones in stratigraphic sequences (after [36]).

Khramov's [37] investigation focused on the magnetic polarity stratigraphy in Pliocene-Pleistocene sediments from western Turkmenistan (Central Asia). He carried out chronostratigraphic interpretations based on the equal time of polarity intervals. Picard [38] successfully applied magnetostratigraphic studies to Triassic red sandstones of the Chugwater Formation (Wyoming, USA). Irving [39] discovered the Kiama paleomagnetic zone of inverse polarity in the Upper Paleozoic in Australia and defined its interrelation with covering the Illawarra zone of normal polarity. This discovery has played a crucial role in subsequent paleomagnetic investigations [26].

The development of the first paleomagnetic maps was associated with mapping the ocean bottoms, where a series of direct and inverse magnetization zones were interpreted as spreading zones [40,41]. In the current stage, the paleomagnetic ocean reconstructions include stages from the Cretaceous and Cenozoic [42] to the Middle Jurassic [43,44]. McDougall et al. [45] demonstrated an effective integration of the paleomagnetic-radiometric data analysis to examine basaltic formations in western Iceland.

Several examples of paleomagnetic zonation of sedimentary deposits in the Volga-Ural and Caucasus regions (Russia) were displayed in [27,46]. Paleomagnetic mapping of the volcanogenic association of the Miocene traps of Transcarpathia was presented in [47].

Kissel and Laj [25] demonstrated the geodynamic paleomagnetic zonation with examples from the easternmost Mediterranean, New Zealand, the USA, and some other regions. Opdyke and Channel [26] presented various generalizations for paleomagnetic mapping. Kristjansson and Jonsson [48] significantly extended the perspectives of paleomagnetic mapping in Iceland. Goguitchaichvili et al. [49] have reliably mapped the Gilbert–Gauss geomagnetic reversal in the Pliocene volcanic sequences in the Lesser Caucasus.

Nur et al. [50] carried out the initial geodynamic paleomagnetic zonation of the transition zone from ocean to continent in northern Israel. The mentioned authors revealed several tectonic blocks of the predominant counterclockwise rotation. Granot et al. [51] employed paleomagnetic mapping in the Troodos gabbro massif (Cyprus) for estimation of the oceanic earth's crust block rotation. Rolland [52] has skillfully applied paleomagnetic mapping to unmask the Caucasian collisional history.

Eppelbaum et al. [18,19] have applied the integrated paleomagnetic-radiometric and magnetic analyses for the tectonic-structural reconstructions in the Sea of Galilee area. As a result, the first magnetic–paleomagnetic–radiometric map (scheme) for this area was developed.

The combined magnetic-paleomagnetic analysis enabled the discovery of the Kiama zone of inverse polarity in the easternmost Mediterranean [31]. This research triggered the development of the first paleomagnetic map of the easternmost Mediterranean based on the integrated interpretation of different geophysical fields and comprehensive analysis of the surrounding sedimentary and volcanogenic structures [22,32,33,53].

Paleomagnetic-geodynamic mapping [22,31] of the easternmost Mediterranean, located between the boundaries of Laurasia and Gondwana, where the Eurasian, Aegean-Anatolian, Nubian, Sinai, and Arabian plates converge, made it possible to clarify and substantiate the location and nature of their crust. For the first time, ophiolite exposures in the distal regions of the foreland adjacent to the southern Tethys zone were identified and mapped. A new tectonic map of the region has been compiled, where the Mesozoic Terrane Belt (MTB) with pre-collision, collision and post-collision traps have been recognized and contoured [22].

The specific complexity of the easternmost Mediterranean follows, first of all, from convergence here collision and spreading processes. A wide range of applied analytical, search and survey methods give a reason to believe that this area can become a reference for mapping techniques for transition zones from the ocean to the continent and geologically complex regions. It makes it possible to test a combination of paleomagnetic-radiometric studies and structural and tectonic analyses.

3. Paleomagnetic Mapping and Profiling in Northern Israel

The combined paleomagnetic mapping has been performed for the following geologically complex areas in northern Israel (see contoured areas in Figure 1): (1) Mt. Carmel and surrounding areas and (2) Atlit area as part of the Mt. Carmel paleomagnetic map (it was caused by the high complexity of the map mentioned above), (3) Sea of Galilee and its vicinity, and (4) Hula Basin and adjacent areas. The paleomagnetic profiles developed across the Carmel—Galilee region (*II–II′*) and across the Hula Valley—Sea of Galilee—Hula Basin (*I–I′–I″*) unmask nontrivial geological sections of these areas.

3.1. Paleomagnetic Maps of Carmel and Atlit Areas

The Mt. Carmel structure (see Figure 1) differs from other coastal plain structures of the easternmost Mediterranean by numerous geological-geophysical characteristics [17,54–58].

The Carmel structure is located at the boundary between the Galilee-Lebanon and Judea-Samaria terranes [6]. Neotectonically, this boundary coincides with the zone of seismic activity within the Yagur fault branch system; it continues onshore and divides the area into the southern and northern sectors [59]. The most recent analysis shows that this boundary is displaced a few km south of the Atlit fault zone [57].
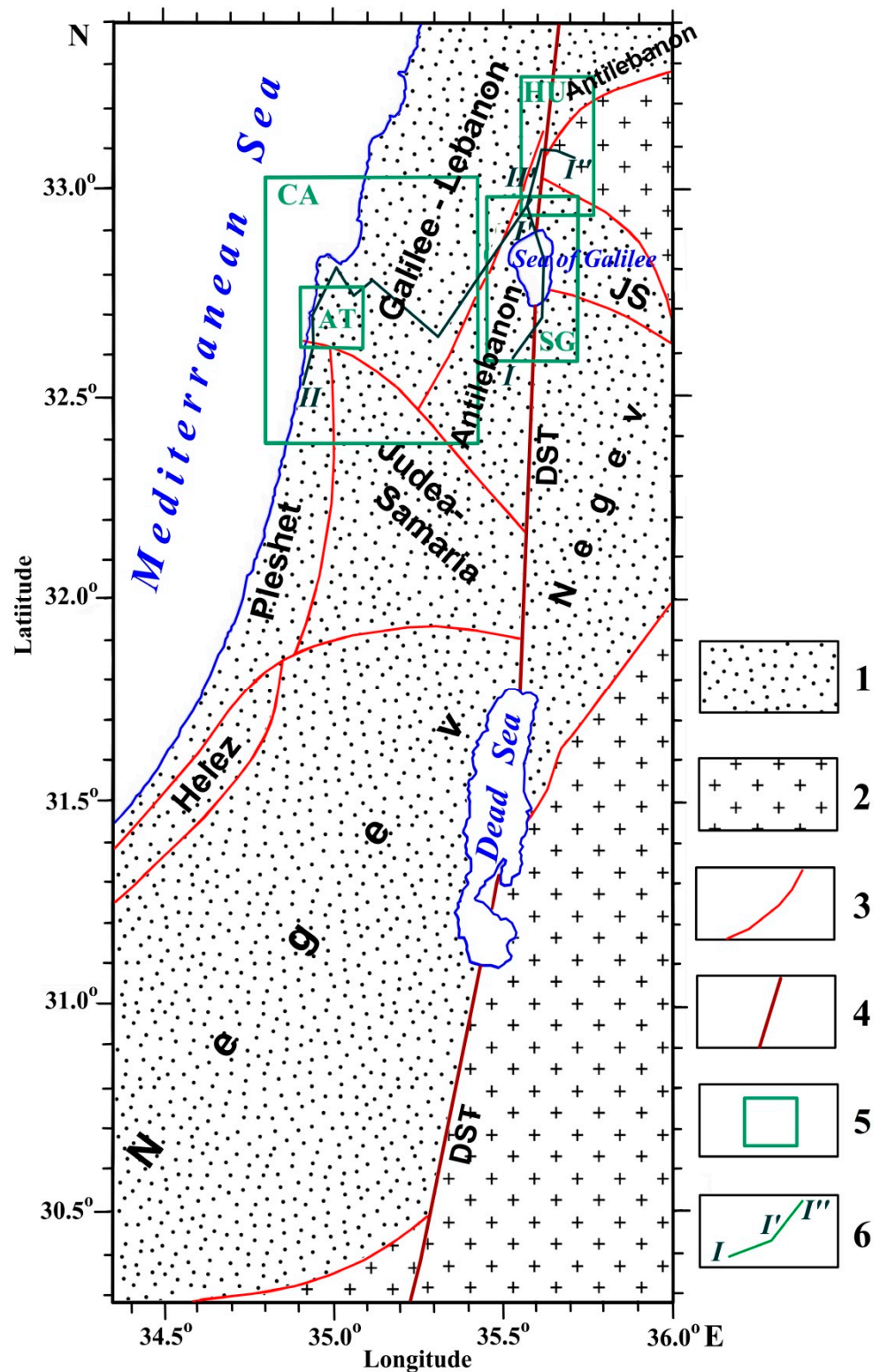
Figure 1. Very simplified structural map of with location of areas of paleomagnetic-radiometric generalization and examined magnetic anomalies. (1) Mesozoic Terrane Belt, (2) Neoproterozoic Belt, (3) intraplate faults, (4) interplate Dead Sea Transform (DST), (5) paleomagnetically investigated areas: CA, Carmel, AT, Atlit, SG, Sea of Galilee (Lake Kinneret), HU, Hula, (6) location of paleomagnetic profiles *I–I′–I″* and *II–II′*. JS, Judea-Samaria.

The Carmel tectonic system plays an essential role in estimating the spatial interaction of the continental and oceanic zones in this area. The oldest discovered deposits are Triassic strata, overlying series of the magmatic and sedimentary rocks of the Early Mesozoic (Asher Volcanics) [60]. The last associations covered by younger Mesozoic-Cenozoic deposits are affected by the prolonged complex deformation of the postaccretional tectonic stage (>130 Ma).

Gvirtzman and Steinitz [60] and Garfunkel [61] assumed that the Early Mesozoic formation of the Asher Volcanics was generated within the graben structure. Gvirtzman et al. [54] suggested that the formations composing this graben have a predominantly continental genesis, including soils and coal. According to other data [62,63], the Asher Volcanics relate to a deep basin with a possible ocean-like crust; the results of our investigation [22,31,32] partially agree with the last proposition.

Discovering numerous mantle minerals [58,64–69] also confirmed the mentioned suggestion. The anomalously high content of the Permian zircons was found in the xenoliths of the Cretaceous volcanoes [65]. Based on the analysis of the ratios of trace elements, the authors mentioned above believed that these zircons are associated with the magmatic complexes of the Earth's crust of the oceanic type.

In the current work, we have expanded the areas of paleomagnetic mapping of the northern part of the easternmost Mediterranean by the attraction of the well-studied geological-geophysical area of the Mt. Carmel and the Sea of Galilee and adjacent areas (Figure 2).

Figure 2 indicates a significant differentiation in the direction of tectonic-thermal processes from the Late Mesozoic to the Late Cenozoic. This testifies to the extreme geodynamic instability of this region and the variety of manifestations of tectonic movements, magmatic processes, and surface relief with the formation of faults, strike-slip valleys, and rotational structures. The dominant direction of the isopachs of the Lover Cretaceous traps of the Halal-1 paleomagnetic superzone corresponds to the NNE-SSW. It is 60° counterclockwise as opposed to the development field of the Upper Cretaceous volcanoes of the Halal-2 superzone—NNW-SSE. Meanwhile, it is 30° counterclockwise compared to the long axis of the Late Cretaceous traps [56] of Mt. Carmel. These data confirm the regional rotation of the deep mantle structure below the Eastern Mediterranean [16] over a long geological time. Diagonal and arc faults oppose the boundaries of larger tectonic blocks (terranes). These fractures, in recent times, have created fault and strike-slip valleys and coastal zones of marching.

The Atlit paleomagnetic map (Figure 3) occupies the central-northern part of the Carmel paleomagnetic map.

Tectonically, this area belongs mainly to the Galilee-Lebanon terrane and the marginal parts of the Pleshet, Judea-Samaria, and Antilebanon terranes (Figure 3). Geophysically, this area is significant in developing the Carmel regional magnetic-gravity anomaly [55]. The anomaly apical part almost coincides with the top part of the Carmel Plateau, with hypsometric elevations of up to 546 m. The Carmel anomaly marks the southern part of the Galilee-Lebanon terrane, where significant differences in the basement depth [55] and developed ophiolite sheets were found. The latter enclose the magmatic complexes and mélange [22].
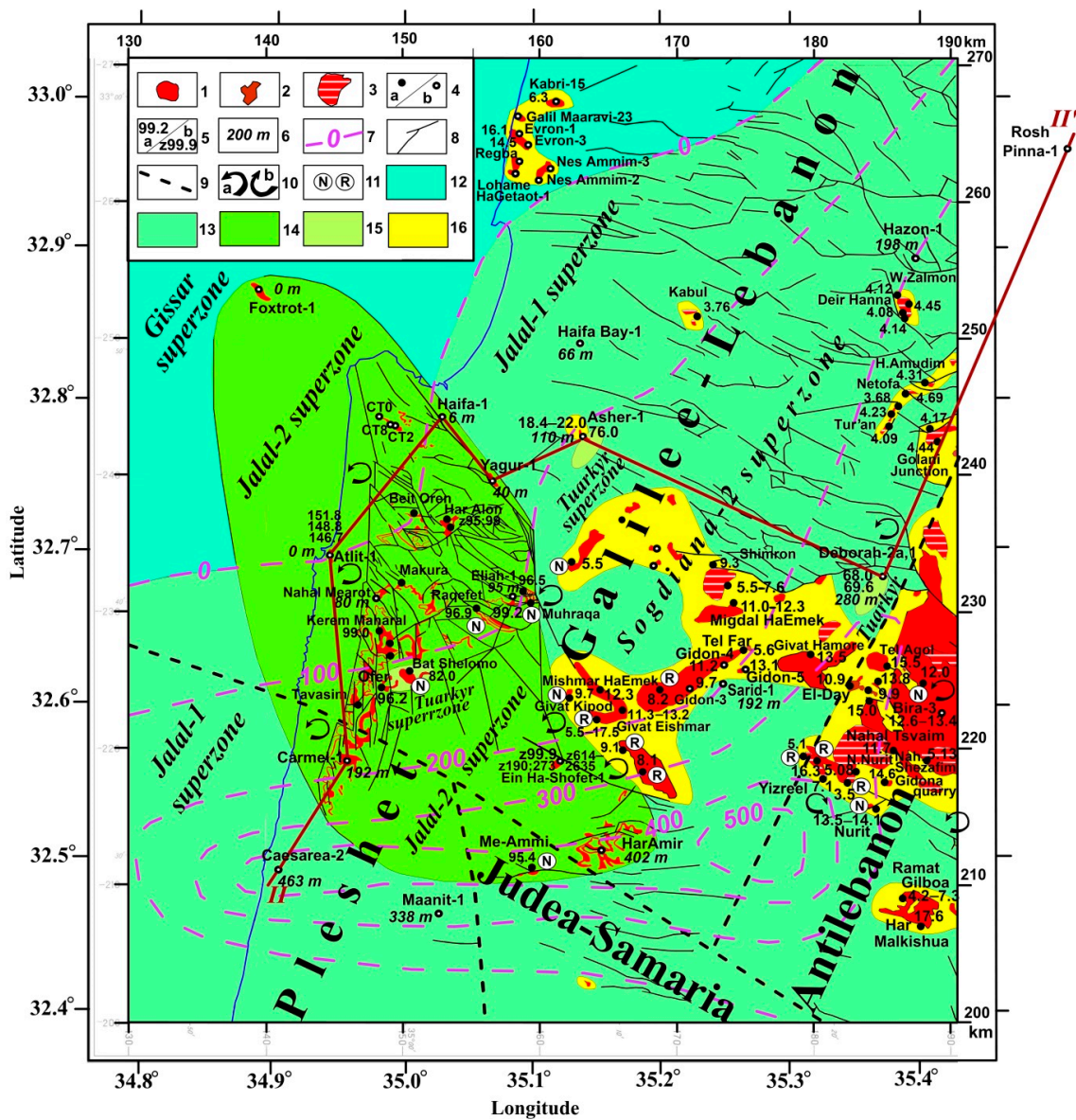
Figure 2. Geodynamic-paleomagnetic map of the Mt. Carmel—Galilee region, CA (see its location in Figure 1). (1) Cretaceous-Miocene basalts, (2) Miocene gabbroid intrusive, (3) Pliocene Cover basalts, (4) outcrops (a) and boreholes (b) with the Mesozoic-Cenozoic magmatic complexes, (5) radiometric age of magmatic rocks and minerals from K-Ar, Ar-Ar methods (a) and zircon geochronology (b), (6) thickness of the Lower Cretaceous traps (in m), (7) isolines of the Lower Cretaceous traps thicknesses (in m), (8) faults, (9) boundaries of terranes, (10) counterclockwise (a) and clockwise (b) rotation derived from tectonic and paleomagnetic data, (11) data of paleomagnetic measurements of magmatic rocks with normal *N* and reverse *R* polarities, (12–15) paleomagnetic zones: (12) Gissar, (13) Jalal-1, (14) Jalal-2, (15) Tuarkyr, (16) Sogdiana-2. The bold brown line shows the location of the paleomagnetic profile *I–I'*. The following main works were used for this map construction: [22,23,50,57,64,65,70–88].

Applied paleomagnetic mapping (profiling) became possible due to new paleomagnetic, radiochronological, mineral, and petrological data and novel structural-tectonic reconstructions. The Gissar and Jalal-1 superzones were derived from the sections of multiple boreholes (e.g., [89]), where the thicknesses and the radiometric ages are accomplished. The geological boundaries of the Gissar and Jalal-1 superzones correspond to the pinching out of collisional-post-collisional effusive trap strata reaching a thickness of 463 m (Caesarea-3 borehole).
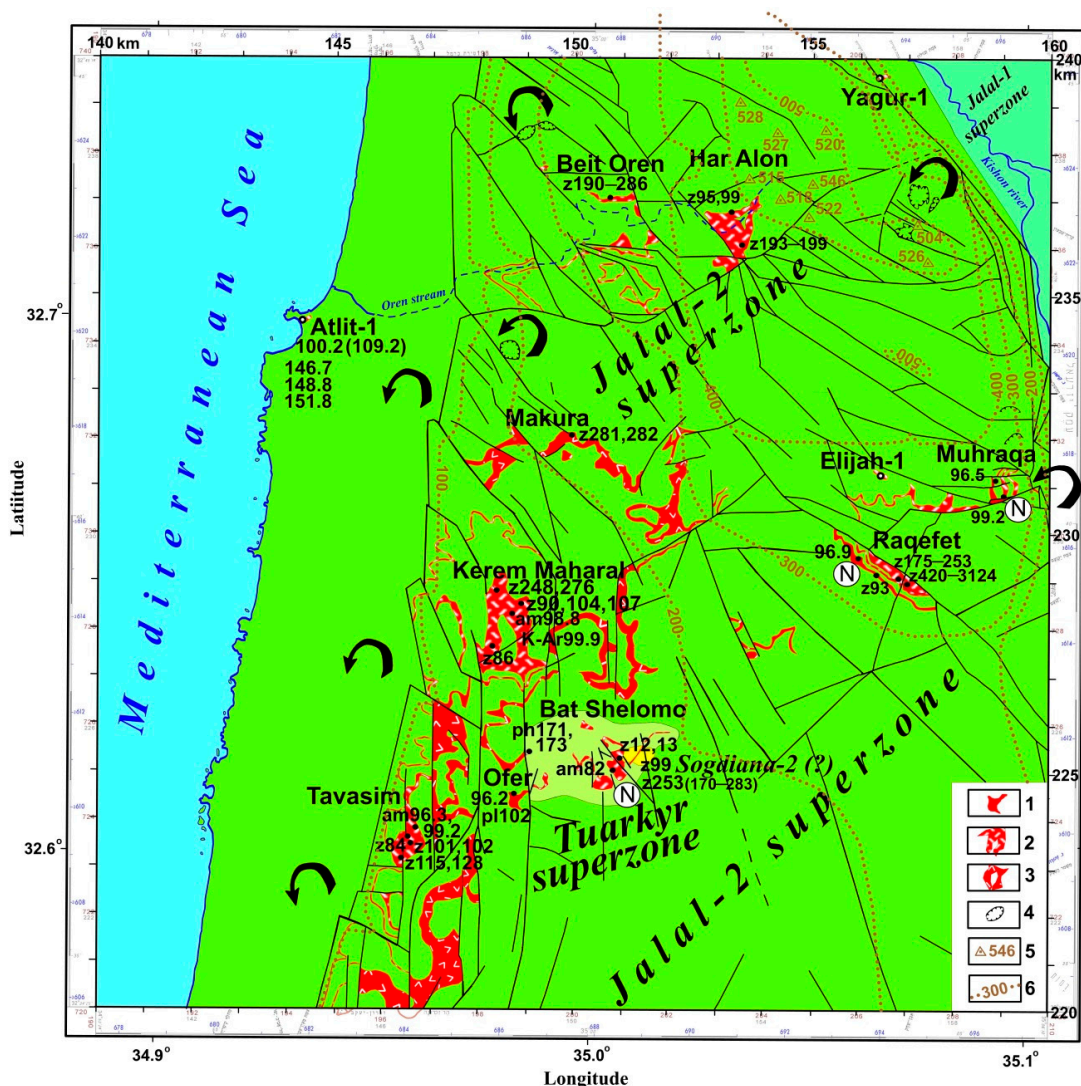
Figure 3. Geodynamic-paleomagnetic map of Atlit area (AT), the middle part of the Carmel area (see its location in Figure 1). This map was developed based on a geological map [57]. (1) basalt lava flows, (2) basalt tuffs, (3) tuffs and flows of basalt volcanic units, (4) landslide scars, (5) highest hypsometric marks, and (6) hypsometric lines.

Stratigraphic and radiometric data from the natural outcrops and Foxtrot-1, Eliah-1, Carmel-1, and Ein Ha-Shofet wells [57,79,90] indicate the development of the Upper Cretaceous (Cenomanian) diamondiferous volcanics [65] of the Jalal-2 superzone. It is pretty indicative that the outline and dimensions of the outcropping area of the paleomagnetic Jalal-2 superzone generally coincide with both magnetic [17,55,91] and gravity [17,55] anomalies of the Mt. Carmel and its outskirts.

The data mentioned above join the deep-geophysical mechanisms of different levels—the mantle plumes from the deep mantle and the movements of the basement of the Earth's crust, which are sources of the shallow anomalies in the gravity and magnetic fields [16,92]. The Tuarkyr paleomagnetic zone (confined in this area to the Senonian), was developed in the form of the insignificant domains at the surface as scattered outcrops of the Bat Shelomo effusive rocks in the south of the Carmel Plateau with the radiometric age of 82 Ma [90].

The other two finds in this superzone are associated with the radiometrically dated sills from the Asher-1 borehole [82] and tuffs from the Devorah-2 borehole [72]. These finds correspond to the Campanian and Maastrichtian, respectively. Paleomagnetic research [80] indicated that a normal polarity characterizes the Late Cretaceous volcanic rocks outcrop-

ping in a few areas. These rocks correspond to the Jalal-2 and Tuarkyr paleomagnetic superzones.

The Sogdiana-2 paleomagnetic superzone, concerning more ancient Mesozoic superzones, extends submeridionally and occurs discordantly. It ranges from the giant outcrop of the Cenozoic Ash Shaam traps diagonally stretching from the SE to the NW. In this area, the belt of the Cenozoic traps forms the scattered outcrops within the Cretaceous and Paleogene rocks and often combines with them in a narrow space (e.g., in the Asher-1 borehole [82]). The Cenozoic traps even used the ancient faults and volcanic apparatus to intrusion into the Mesozoic traps, as discovered [65] in the Santonian Bat Shelomo volcano field.

3.2. Paleomagnetic Profile across the Carmel-Galilee Region

The paleomagnetic profile crosses the area of the Mt. Carmel, Northern Galilee, and the Korazim Plateau of the DST region (north of the Lake Kinneret), from SW to NE from the Pleshet terrane through the Galilee-Lebanon terrane to the Antilebanon terrane (Figure 4; see location of this profile in Figure 1).
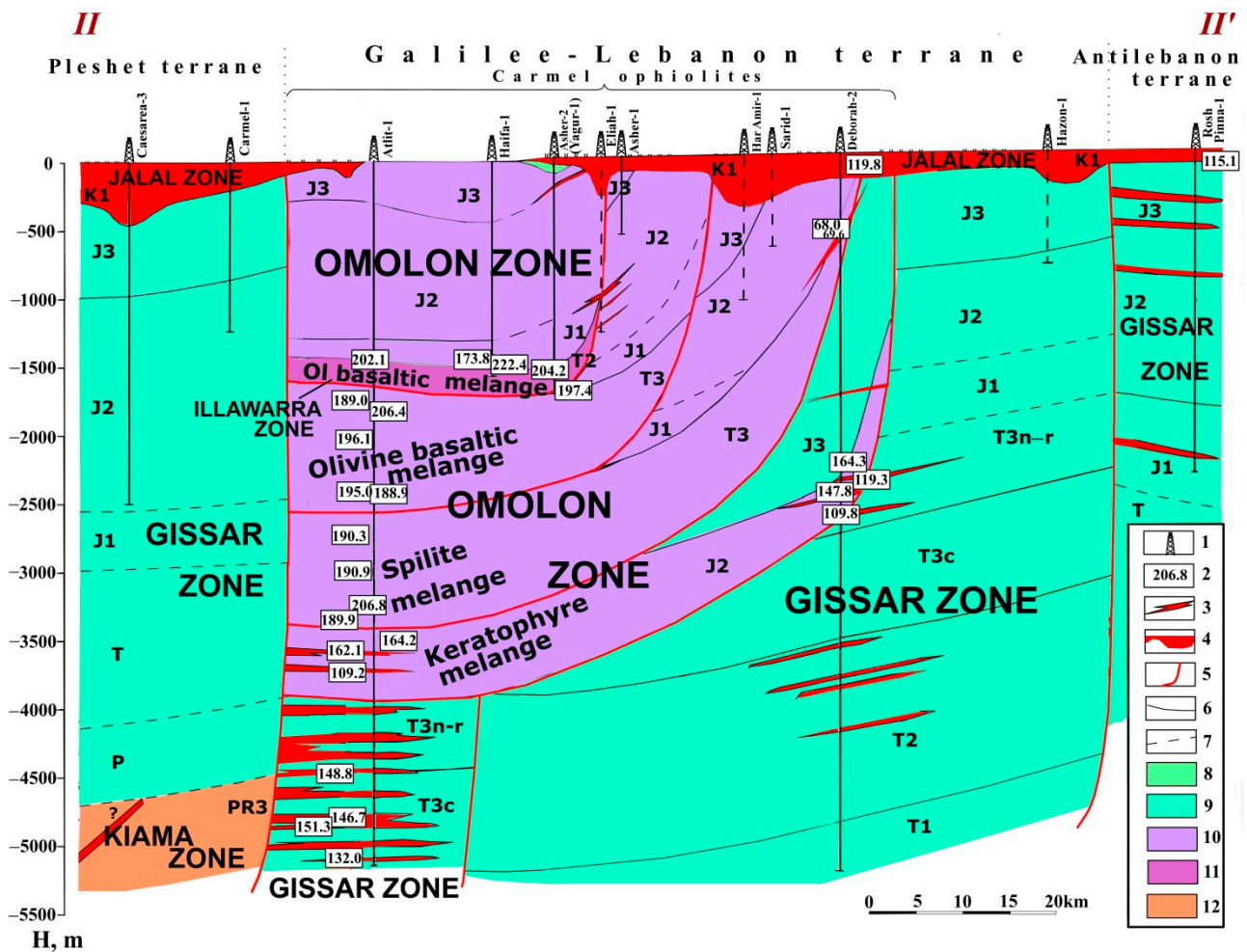

Figure 4. Paleomagnetic profile *II–II′* of the Carmel-Galilee region along the top of the accumulative surface of the Lower Cretaceous traps (location of this profile is shown in Figures 1 and 2). (1) borehole, (2) radiometric age, (3) dykes and sills, (4) traps, (5) faults, (6) established stratigraphic boundaries, (7) supposed position of the stratigraphic boundaries, (8–12) paleomagnetic zones: (8) Jalal, (9) Gissar, (10) Omolon, (11) Illawarra, (12) Kiama. The following main works were used for this map construction: [32,54,55,60,61,63,78,89].

The Pleshet and Antilebanon terranes are somewhat uplifted tectonically than the Galilee-Lebanon terrane. This profile is constructed along the top of the accumulative leveling surface of the Lower Cretaceous traps belonging to the Jalal-1 paleomagnetic zone (131–105 Ma).

The underlying Triassic-Jurassic sequences that make up the cover of the MTB carbonate platform contain dikes and sills of Tithonian-Neocomian basaltoids (132–153 Ma) and belong to the Gissar paleomagnetic zone. Concerning the terranes themselves, the carbonate platform represents an autochthonous complex; however, both carbonates and intrusive traps were formed in the pre-collision stage, when the terranes bordered the southern part of the Neotethys Ocean at the boundary with the Gondwana foreland. The profile testifies that an allochthonous complex of ophiolites, occurring above the carbonate platform, has developed in the Galilee-Lebanon terrane. It forms four sheets of different ages. The lowest of them, the youngest, is composed of keratophyre mélange aged 162–164 Ma (Omolon paleomagnetic zone) and is covered with relatively deep-water Upper Jurassic carbonates penetrated by intrusive traps of the Gissar zone. Two middle ophiolite plates are composed of spilite and olivine-basalt mélange (188–206 Ma) and deep-water Jurassic carbonates and generally belong to the Omolon paleomagnetic zone. Finally, the upper ophiolite plate, the oldest, 197.4–222.4 Ma, is composed of basalt mélange and covered with Jurassic carbonates (174 Ma). This age generally corresponds to the Illawarra-Omolon paleomagnetic zones (Figure 4).

The dynamics of sequential attachment of ophiolite sheets during collision and shear movements of oceanic plates and the Galilee-Lebanon terrane during the Levantine phase of tectogenesis at the boundary of the Early and Late Hauterivian was considered earlier [77]. These authors have shown that the amplitude of horizontal displacements of ophiolite plates could reach 120 km.

3.3. Combined Paleomagnetic-Radiometric Scheme of the Sea of Galilee and Its Vicinity

The region of the Sea of Galilee (Lake Kinneret) is a reference object for the paleomagnetic mapping transition regions from the ocean to the continent in terms of structural, historical-geological, and methodological approaches. The uniqueness of this target is because here developed the phenomena and structures of the collisional type caused by the closure of the Neotethys Ocean and the elements of the initial phases of the Red Sea—East African Rift system spreading.

It has long been used as the largest freshwater reservoir in the Middle East and as an etalon region for monitoring and accounting for seismicity in the area of active housing construction and areas of industrial and agricultural facilities development.

There are several fault systems in this area, the main ones being the N–S transform system and the E–W and NW–SE fault systems that break up the Galilee. The sea, and the plain to its south, are located in a depression bounded on the east and west by active fault scarps with steep gradients [93]. The superposition of vertical displacements perpendicular or oblique to the transform impedes structural interpretation of the investigated basin [94].

At the end of the twentieth century, various geological and geophysical surveys raised the question of developing a generalizing tectonic-geodynamic model (e.g., [94]). Further studies [18,19,22] showed that the optimal linkage consists of integrating the methods of magneto-geophysics (adopted in the study of the oceans) and paleomagnetic stratigraphy (assumed for the continents), combined with independent geological-geophysical investigations. The developed map (Figure 5) also contains the revised and generalized results of the quantitative interpretation of numerous magnetic anomalies in the Sea of Galilee [19].
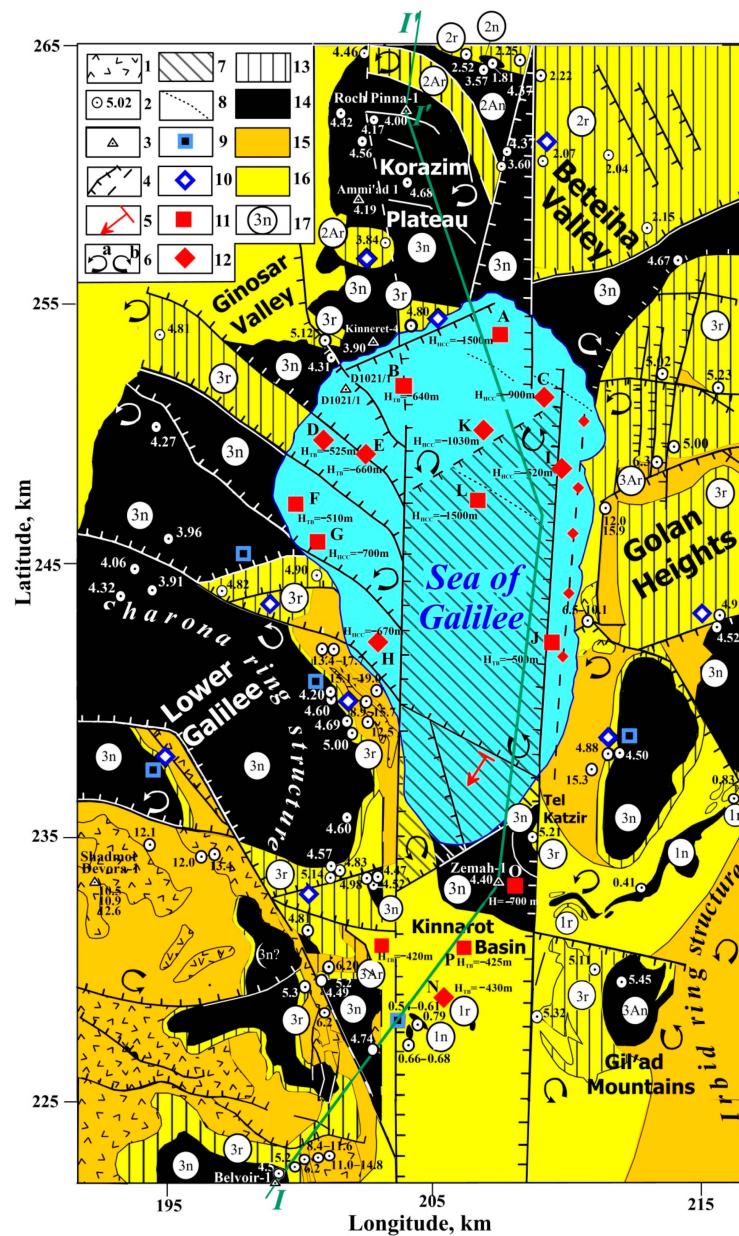
Figure 5. Integrated paleomagnetic scheme of the Sea of Galilee, SG (see its location in Figure 1). (1) outcropped Cenozoic basalts, (2) points with radiometric age of basalts (in Ma), (3) boreholes, (4) faults, (5) general direction of the proposed buried basaltic plate dipping in the southern part of the Sea of Galilee, (6) counterclockwise (a) and clockwise (b) rotation of faults and tectonic blocks, (7) pull-apart basin of the Sea of Galilee, (8) suggested boundaries of the paleomagnetic zones in the sea, data of land paleomagnetic measurements: (9 and 10) (9) reverse magnetization, (10) normal magnetization, (11 and 12) results of magnetic anomalies analysis: (11) normal magnetization, (12) reverse magnetization, (13) reversely magnetized basalt fields, (14) normal magnetized basalt fields, (15) Miocene basalts and sediments with complicated paleomagnetic characteristics, (16) Pliocene-Pleistocene basalts and sediments with complicated paleomagnetic characteristics, (17) index of paleomagnetic zonation. Tectonic setting after [76,94–98]. 1n, 2n, 3n, 1Ar, 2Ar, and 3Ar are the indexes of paleomagnetic zones. Radiometric data (K-Ar and Ar-Ar) after [73,75,97,99,100]. Paleomagnetic data after [70,73–75,85,95,97,99,101–103]. H_{TB} and H_{HCC} designate the calculated depths of basaltic bodies in the basin: H_{TB} is the upper edge for the model of the thin bed, H_{THP} is the upper edge for the model of the thin horizontal plate, and H_{HCC} is the center for the model of the horizontal circular cylinder. The bold green line designates the location of paleomagnetic profile $I–I'$.

It was the first experience of such research in the transition areas from the ocean to the continent. In the context of the regional geological-geophysical studies of the African-Arabian region, paleomagnetic mapping of the area of the Sea of Galilee has been significantly expanded and detailed [16,23,32,53].

The supplemented edition of the paleomagnetic map of the Sea of Galilee (Figure 5) was extended to the south, where the Belvoir uplift has developed. Here, the data from a drilled deep well and numerous radiometric data of the Cenozoic traps were analyzed. The essential revision of this map is based on the attraction of new data from structural, radiometric, and paleomagnetic analyses, which expanded understanding of the studied area's structure and development.

In such a manner, we nailed the mapping of the transition region from the ocean to the continent to the methods widely used in the paleomagnetic mapping of the marine areas [22], and optimally compiled with the geodynamic principles [25]. A novel variant of the paleomagnetic map of the Sea of Galilee and adjacent areas (Figure 5) includes an anomalous pull-apart basin, areas of development of the circular structures [16,22], the arc faults, and the rotational markers of the crustal blocks identified from the structural and paleomagnetic data [94–96].

Here, two comparatively large ring structures are presented. The first is the Sharon trap depression located in the central-western part of the map. The second is the Irbid ring structure, bounded by conical dikes and partially presented in the southeastern area. Significantly, the largest amplitude of rotation is 58° counterclockwise, registered in the Sharona ring structure (Figure 5), which emphasizes the complexity of the geodynamics of the trap genesis zone. A different nature has an Irbid ring structure also prone to counterclockwise rotation (Figure 5).

3.4. Hula Paleomagnetic Map

In the extreme west of the district, in the Upper Galilee Heights, Upper Cretaceous and Paleogene sedimentary formations related to the Khorezm-Tuarkyr and Jalal paleomagnetic superzones were mainly developed. In the northeast, on the slope of the Hermon Mt., Jurassic and Cretaceous formations penetrated by pre-collisional, collisional, and post-collisional traps of the Gissar and Jalal superzones were developed (Figure 6).

Due to the paleomagnetic mapping methodology elaboration in the etalon area of the Sea of Galilee, it became possible to construct a paleomagnetic map of its northern extension—Hula Valley (Figure 6). The constructed map also includes areas of the Upper Galilee Heights, the northern slope of the Korazim Plateau, the northern part of the Golan Plateau, and the southern side of the Hermon Mts. The area comprises mainly the Pliocene-Quaternary traps and the sedimentary complexes belonging to the Brunhes-Matuyama zones. More ancient Pliocene trap complexes were developed to the south, in the Korazim Plateau and Beteiha Valley. These complexes belong to the Gauss and Gilbert paleomagnetic superzones.

In the extreme west of the district, in the Upper Galilee Heights, mainly Upper Cretaceous and Paleogene sedimentary formations developed. They relate to the Khorezm-Tuarkyr and Jalal paleomagnetic superzones. Jurassic and Cretaceous formations developed in the northeast on the slope of the Hermon Mt., penetrated by pre-collisional, collisional, and post-collisional traps. The latter relates to the Gissar and Jalal paleomagnetic superzones (Figure 6).

3.5. Paleomagnetic Profile Kinnarot Valley—Hula Basin

Without bringing it to Hermon, we slightly turned the profile line to show the structural contrast of the Antilebanon terrane with the Neoproterozoic base of Gondwana, which composes the lower structural levels of the northern part of the Golan Plateau. Here the Gissar, Jalal, and Sogdiana paleomagnetic superzones are sharply reduced in thickness compared to their analogs in the Antilebanon terrane. Within the blocks of the Gondwana oneself, there are almost no chalk traps developed. The complexity of the structure of the

Kinneret and Hula depressions becomes evident in the constructed paleomagnetic profile *I–I'–I''* (Figure 7).
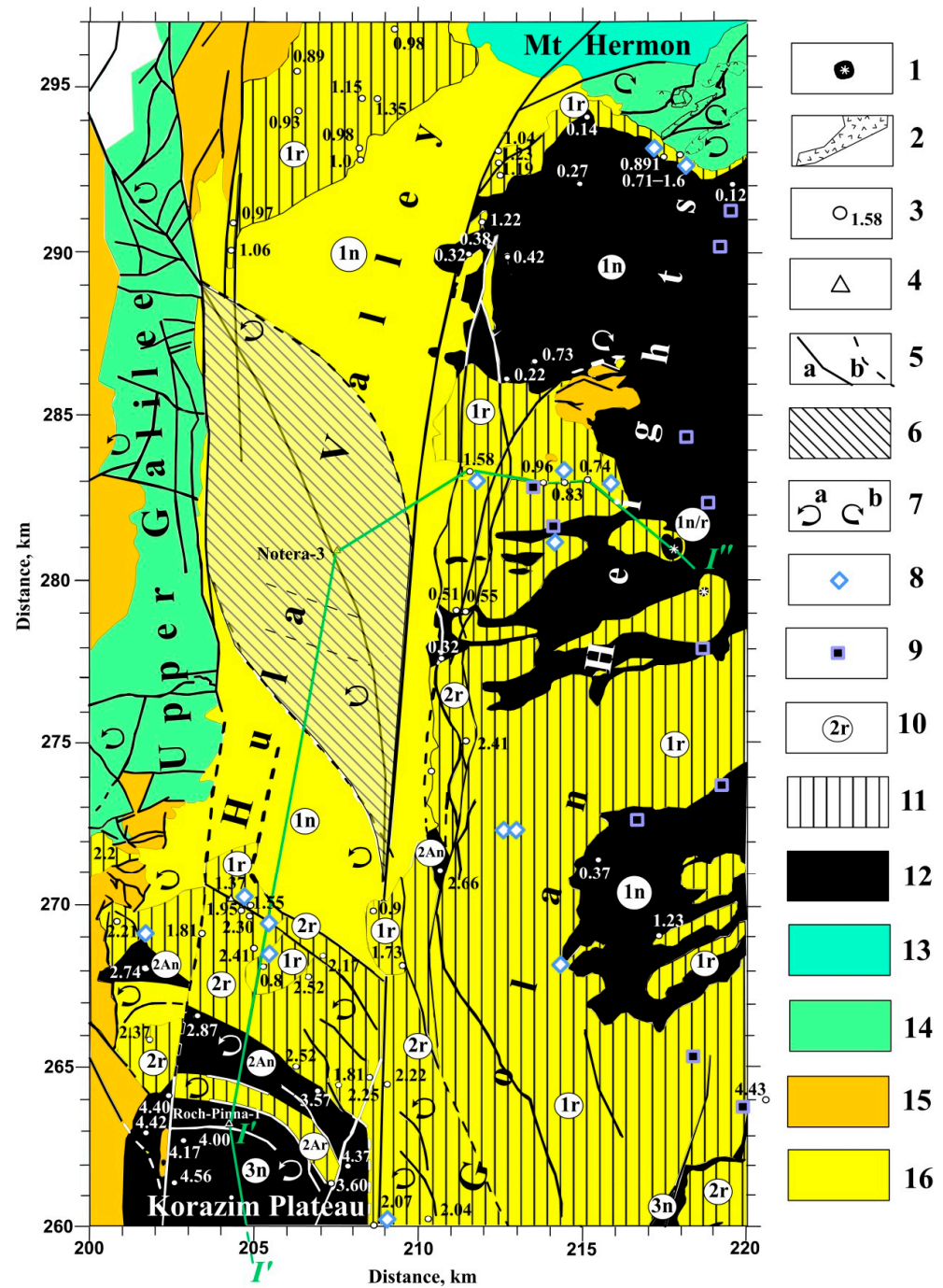

Figure 6. Paleomagnetic-geodynamic map of the Hula Basin and adjacent areas of the Golan Plateau, Hermon Mt., and Galilea uplift, HU (see its location in Figure 1). (1) volcanic cones, (2) Cretaceous traps, (3) outcrops with the radiometric ages of basalts (in Ma), (4) boreholes, (5) faults: (a) observed, (b) reconstructed, (6) pull-apart basin, (7) tectonic blocks rotations: (a) counterclockwise, (b) clockwise, (8) outcrops with the determined reversely magnetized basalts, (9) outcrops with the determined normally magnetized basalts, (10) chrons of Geomagnetic Polarity Timescale, (11) areas of the reversely magnetized basalts, (12) areas of the normally magnetized basalts, (13) Gissar superzone, (14) Jalal superzone, (15) Tuarkyr—Khorezm superzone, (16) Sogdiana superzone. Tectonic setting after: [76,97,104–106]. Radiometric data (K-Ar and Ar-Ar) after: [73,74,78,90,97,107]. Paleomagnetic data: [74,75,85,95,97,101]. The bold green line designates the location of paleomagnetic profile *I'–I''*.
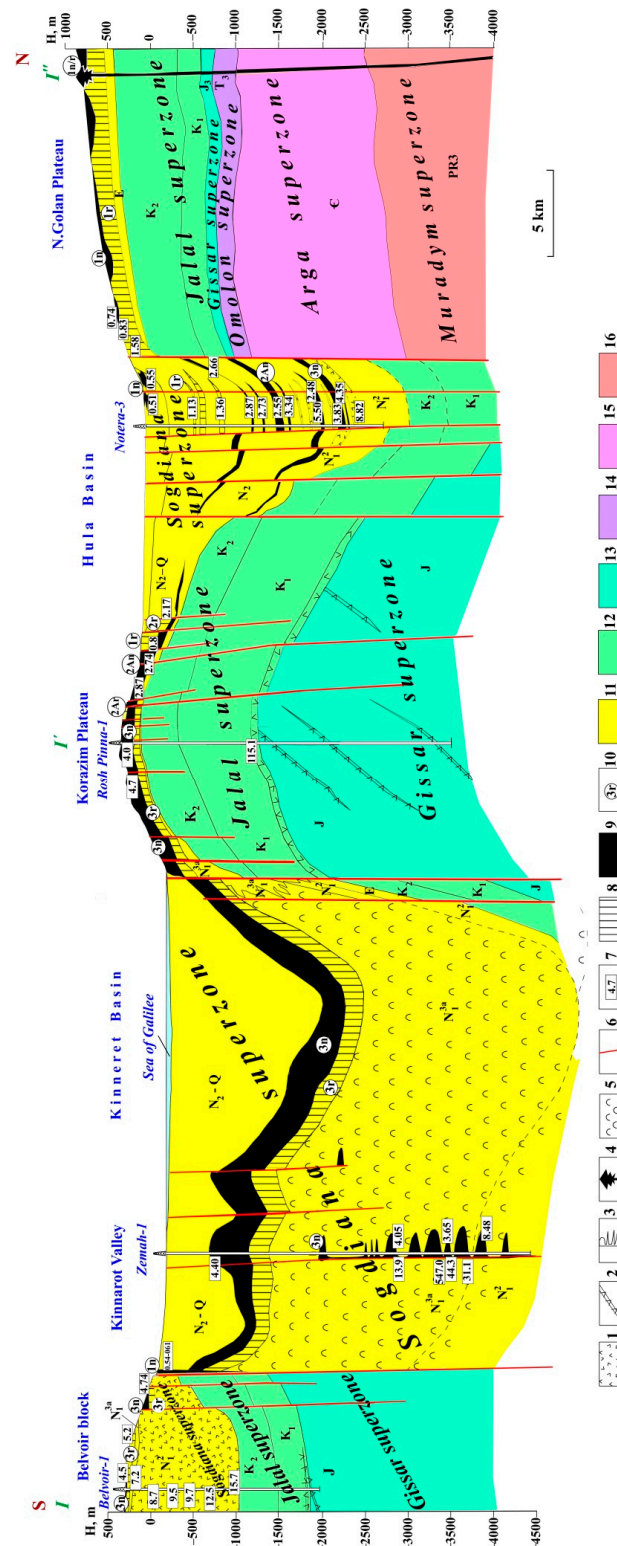
Figure 7. Paleomagnetic profile Kinnarot—Hula (its location is shown in Figures 1, 5 and 6). (1) basic traps, (2) basic dykes, (3) gabbro, (4) volcanic cones, (5) evaporite sediments, (6) faults, (7) radiometric dating, (8) reversal polarity, (9) normal polarity, (10) indexes of Plio-Pleistocene paleomagnetic scale, (11) Sogdiana superzone, (12) Jalal superzone, (13) Gissar superzone, (14) Omolon superzone, (15) Arga superzone, (16) Moradym superzone. The primary utilized sources (besides publications presented in captions for Figures 5 and 6) are: [33,100].

It stretches from the north to the south for more than 60 km. The southwestern and northeastern extremities of the profile are located about 20 km in latitude (Figures 5 and 6).

The deep structure is elicited from the regional tectonic constructions [15,32], results of seismic profiling [104,108,109], boreholes data [89,110], regional geological map [76], radiometric data [73,75,97,105,107]; and the results of the paleomagnetic zonation [16,18,19,22].

Structurally, the paleomagnetic profile corresponds to three uplifts: Belvoir, Korazim, and Golan, between which there are two depressions—Kinneret-Kinnarot and Hula. The first two uplifts and depressions are formed within the southern block of the Antilebanon terrane (Figure 1), shifted relative to the northern one uplifted block of the higher Hermon plateau along the Dead Sea Transform (DST) for about 100 km.

The Kinneret-Kinnarot and Hula are the pull-apart basins with the different amplitudes of subsidence of the Late Cenozoic sedimentary formations. Both the basins contain the traps related to the Sogdiana paleomagnetic superzone.

Without bringing it to Hermon, we slightly turned the profile line to show the structural contrast of the Antilebanon terrane with the Neoproterozoic base of Gondwana, which composes the lower structural levels of the northern part of the Golan Plateau. Within the blocks of the Gondwana oneself, there are almost no chalk traps developed. They are concentrated mainly in the MTB area [100,111].

4. Discussion and Conclusions

The presence of hard explained phenomena of magneto-geophysics prompted combined paleomagnetic-radiometric mapping to reveal the geodynamics history based on the paleomagnetic age reconstruction. The applied mapping includes the procedures for paleomagnetic determination of age and the typification of the magnetized objects, making it possible to widely use the plate geodynamics concepts. It enables the description of the stages of development of various forms of magmatism under transition from the ocean to the continent. The broad integration of paleomagnetic mapping with other geophysical and geological methods significantly increases the efficiency of its application.

Tectonic-paleomagnetic mapping as a new type of geological-geophysical survey contributed to the necessary amendment to the understanding of the nature and structure of the easternmost Mediterranean. The studied areas in northern Israel: Carmel, Atlit, Sea of Galilee, and Hula Basin, are unique objects from the geological point of view, and they are well investigated in various ways. However, their structure, geodynamics, and other critical questions of genesis are not clear and inexplicable. Therefore, we decided to apply the combined paleomagnetic mapping to investigate these intricate targets.

Interestingly, for the mapping examination, a wide diapason of the paleomagnetic data was used: from the Paleozoic (Permian—Carboniferous)—Kiama paleomagnetic superzone in the easternmost Mediterranean [31] to the Holocene—almost modern volcano with a lake in the Birkat Ram crater in the Golan Heights [101]. Without hesitation, this study became possible only thanks to the many years of painstaking work of Israeli geologists and geophysicists, who created a vast database of paleomagnetic (e.g., [50,70,73–75,85,95, 97,99,102,103]) and radiometric studies (e.g., [71–74,78,81,90,97,107]), data of geological mapping and tectonic reconstructions (e.g., [10,15,30,54,57,60–62,76,78,79,83,84,86–88,93, 94,97,100,104–106,108]) for the territory of Israel.

After changing the well-developed geosyncline theory to plate tectonics (convective geodynamics) and the decrease in standard geocartographic research worldwide, a methodological vacuum arose with the lack of mapping technology development. Our comprehensive studies in the African-Arabian region on the junction of Eurasia and Gondwana (e.g., [16]) with the application of paleomagnetic mapping techniques are the testing instrument for developing new kinds of combined investigations of geologically complex areas. Our comprehensive studies in the African-Arabian region on the junction of Eurasia and Gondwana (e.g., [16]) with the widespread application of paleomagnetic mapping techniques are the testing instrument for developing new kinds of combined investigations of geologically complex areas.

Paleomagnetic profiling is a very rarely used but effective research method. The paleomagnetic profile constructed along the top of the accumulative leveling surface of the Lower Cretaceous traps (Figure 4) clearly unmasks the geodynamic history of the Carmel-Galilee region. This procedure is practically impossible to implement using other geophysical methods. This profile makes it possible to reveal the significant tectonic and geodynamic differences between the Mesozoic and Cenozoic traps, differing in thickness and partly to the composition. The latter are usually associated not with the collision stage but with the spreading processes in East Africa and the Red Sea [9,15,16,112]. The beginning of the activation of this process 34 Ma ago is associated with a mantle plume near the Afar triangle. In the Narrat Ash Shaam volcanic field, the dikes of the most ancient traps have an age of 22–26 Ma [81], which corresponds to the boundary of the Oligocene and Miocene.

In the more southerly located Makhtesh Ramon area, integrated geological-geophysical data revealed the pre-collisional, collisional, and post-collisional traps [22], which are distinguished in the presented paleomagnetic profile (Figure 7). In the Korazim block (based on the Rosh Pinna-1 borehole data), these traps indicate the Levantine phase of the angular unconformity, which roughly corresponds to the boundary between the Gissar and Jalal paleomagnetic superzones.

Very indicative is the discovery of the xenoliths in the intrusions of Late Miocene—Early Pliocene gabbroids in the deep Zemah-1 well [100], with a radiometric age of 31.1 Ma (Lower Oligocene), 44.3 Ma (Middle-Upper Eocene), and 547 Ma (Precambrian—Lower Cambrian). These ages are also confirmed by the radiometric age of the basic rock pebbles—41.0 Ma from the Middle Miocene Um Sabune conglomerates in the Tabkha area [73] on the southwestern boundary of the Korazim plateau near the Lake Kinneret coast. Data on the older, Eocene trap magmatism in the Arabian Plate is associated with the beginning of the Red Sea rift opening and are novel.

The paleomagnetic profile (Figure 7) demonstrates a structural difference in the study region in the superzones' thicknesses and magmatism types in different structures. This profile also indicates the structural evolution manifested in the degree of activation of specific paleomagnetic units. The increase in these units' thicknesses relates to the boundary of the Jurassic and Cretaceous (Gissar superzone) and the Middle Miocene—Pliocene—Anthropogen (Sogdiana-2 superzone). Thus, the radiometric dating enables substantiating the Sogdiana-1 superzone trap assemblage and the upper part of the Khorezm superzone.

Overall, the paleomagnetic methods have established themselves as a powerful tool for geodynamic mapping. At the same time, optimal integration of paleomagnetic mapping with other geophysical and geological methods significantly increases its effectiveness and significance [22,23].

Based on the research conducted, we can draw the following main conclusions.

The side of the plate tectonics concept confirmed that the dominance of the geodynamics of the region in the Mesozoic and Cenozoic was carried out not from the western (Atlantic) but the eastern (Neothetical) direction. Paleomagnetic mapping (profiling) made it possible to evaluate the previously identified structures of different ranks. It is a novel unified approach due to the optimal combination of different applied geological-geophysical methods.

The area of development of the Sea of Galilee pull-apart basin has been identified, experiencing differentiation under conditions of the left DST shift and the formation of the faults and ring structures rotating counterclockwise in the adjacent zones. This phenomenon was explained at the level of the regional integrated geophysical studies using 3D modeling and structural-geodynamic analysis [92].

Integrated analysis of geological-geophysical data from the Sea of Galilee and Carmel (Atlit) areas indicates that both mentioned terranes and the MTB were moved in the Mesozoic from the east to the west in a counterclockwise direction. The paleomagnetic studies in the Carmel area showed that the Triassic-Jurassic ophiolite complex underlying the Aptian-Albian traps of the Mt. Carmel (within the Galilee-Lebanon terrane) contrasts

sharply with the Mesozoic and sedimentary rocks penetrated by traps. These traps of the Late Jurassic-Neocomian age precede the Late Jurassic-Neocomian phase of joining MTB to the Gondwana.

The paleomagnetic profile constructed in the Carmel-Galilee region along the top of the accumulative leveling surface of the Lower Cretaceous traps is of essential importance: it unmasks key episodes of a complex geodynamic history of the easternmost Mediterranean.

The paleomagnetic profile Kinnarot Valley—Sea of Galilee—Hula Basin distinctly shows different amplitudes of subsidence of the Late Cenozoic sedimentary formations and traps related to the Sogdiana paleomagnetic superzone. First of all, this physical-geological model is essential for the geoecological monitoring of this significant source of fresh water in Israel.

The Cenozoic stage of development in the region looks to be discordant with the paleomagnetic structural zones of the Mesozoic and Cenozoic. This discordance was explained in light of the latest deep-geodynamic studies [16]. The axis of the discovered deep mantle structure [92] in the middle of the Cenozoic began to turn more intensively in the counterclockwise direction. This effect caused the development of the lithospheric plate disruptions, the formation of the topologically displaced dyke complex' zones, and younger effusive traps.

The proposed methodology of advanced paleomagnetic mapping can be effectively applied to solving different geological-geophysical problems in various geologically complex regions of the world.

References

1. McKenzie, D. Active tectonics of the Mediterranean region. *Geophys. J. Int.* **1972**, *30*, 109–185. [CrossRef]
2. Khain, V.E. *Tectonics of Continents and Oceans*; Scientific World: Moscow, Russia, 2001; 606p. (In Russian)
3. Muttoni, G.; Kent, D.V.; Garzanti, E.; Brack, P.; Abrahamsen, N.; Gaetani, M. Early Permian Pangea 'B' to Late Permian Pangea 'A'. *Earth Planet. Sci. Lett.* **2003**, *215*, 379–394. [CrossRef]
4. Stern, R.J.; Johnson, P. Continental lithosphere of the Arabian Plate: A geologic, petrologic, and geophysical synthesis. *Earth-Sci. Rev.* **2010**, *101*, 29–67. [CrossRef]
5. Faccenna, C.; Becker, T.W.; Auer, L.; Billi, A.; Boschi, L.; Brun, J.P.; Capitanio, F.A.; Funiciello, F.; Horvàth, F.; Jolivet, L.; et al. Mantle dynamics in the Mediterranean. *Rev. Geophys.* **2014**, *52*, 283–332. [CrossRef]
6. Ben-Avraham, Z.; Ginzburg, A. Displaced terranes and crustal evolution of the Levant and the eastern Mediterranean. *Tectonics* **1990**, *9*, 613–622. [CrossRef]
7. Le Pichon, X.; Kreemer, C. The Miocene-to-present kinematic evolution of the Eastern Mediterranean and Middle East and its implications for Dynamics. *Annu. Rev. Earth Planet. Sci.* **2010**, *38*, 323–351. [CrossRef]
8. Stampfli, G.M.; Hochard, C.; Vérard, C.; Wilhem, C.; von Raumer, J. The formation of Pangea. *Tectonophysics* **2013**, *593*, 1–19. [CrossRef]
9. Bosworth, W.; Huchon, P.; McClay, K. The Red Sea and Gulf of Aden basins. *J. Afr. Earth Sci.* **2005**, *43*, 334–378. [CrossRef]
10. Ben-Avraham, Z.; Schattner, U.; Lazar, M.; Hall, J.K.; Ben-Gai, Y.; Neev, D.; Reshef, M. Segmentation of the Levant continental margin, eastern Mediterranean. *Tectonics* **2006**, *25*, 1–17. [CrossRef]
11. Picard, L. Geology and oil exploration of Israel. *Bull. Res. Counc. Israel* **1959**, *G8*, 1–30.
12. Ben-Avraham, Z. The structure and tectonic setting of the Levant continental margin, Eastern Mediterranean. *Tectonophysics* **1978**, *46*, 313–331. [CrossRef]

13. Rotstein, Y.; Ben-Avraham, Z. Active Tectonics in the Eastern Mediterranean: The role of oceanic plateaus and accreted terranes. *Isr. J. Earth Sci.* **1986**, *35*, 23–39.

14. Robertson, A.H.F. Mesozoic-Tertiary Tectonic Evolution of the Easternmost Mediterranean Area: Integration of Marine and Land Evidence. In *Proceedings of the Ocean Drilling Program, Scientific Results*; Robertson, A.H.F., Eneis, K.C., Richter, C., Camerlenghi, A., Eds.; Texas A & M University: College Station, TX, USA, 1998; Volume 160, pp. 723–782.

15. Hall, J.K.; Krasheninnikov, V.A.; Hirsch, F.; Benjamini, C.; Flexer, A. Geological Framework of the Levant. Volume II: The Levantine Basin and Israel. In *Geological Framework of the Levant*; Historical Productions-Hall: Jerusalem, Israel, 2005.

16. Eppelbaum, L.V.; Ben-Avraham, Z.; Katz, Y.; Cloetingh, S.; Kaban, M. Giant quasi-ring mantle structure in the African-Arabian junction: Results derived from the geological-geophysical data integration. *Geotectonics* **2021**, *55*, 67–93. [CrossRef]

17. Ben-Avraham, Z.; Hall, J. Geophysical survey of Mount Carmel structure and its extension into the eastern Mediterranean. *J. Geophys. Res.* **1977**, *82*, 793–802. [CrossRef]

18. Eppelbaum, L.; Ben-Avraham, Z.; Katz, Y. Integrated analysis of magnetic, paleomagnetic and K-Ar data in a tectonic complex region: An example from the Sea of Galilee. *Geophys. Res. Lett.* **2004**, *31*, 1–4. [CrossRef]

19. Eppelbaum, L.V.; Ben-Avraham, Z.; Katz, Y.I. Structure of the Sea of Galilee and Kinarot Valley derived from combined geological-geophysical analysis. *First Break* **2007**, *25*, 21–28. [CrossRef]

20. Rybakov, M.; Voznesensky, V.; Ben-Avraham, Z.; Lazar, M. The Niklas anomaly southwest of Cyprus: New insights from combined gravity and magnetic data. *Isr. J. Earth Sci.* **2008**, *57*, 125–138. [CrossRef]

21. Eppelbaum, L.V. Comparison of 3D integrated geophysical modeling in the South Caucasian and Eastern Mediterranean segments of the Alpine-Himalayan tectonic belt. *ANAS Trans. Earth Sci.* **2015**, *3*, 25–45.

22. Eppelbaum, L.V.; Katz, Y.I. Paleomagnetic Mapping in Various Areas of the Easternmost Mediterranean Based on an Integrated Geological-Geophysical Analysis. In *New Developments in Paleomagnetism Research*; Series: Earth Sciences in the 21st Century; Eppelbaum, L., Ed.; Nova Science Publisher: Hauppauge, NY, USA, 2015; pp. 15–52.

23. Eppelbaum, L.V.; Katz, Y.I. Deep Tectono-Geodynamic Aspects of Development of the Nubian-Arabian Region. In *The Arabian Seas Biodiversity, Environment Challenges and Conservation Measures*; Jawad, L., Ed.; Springer: Berlin/Heidelberg, Germany, 2021; pp. 199–237. [CrossRef]

24. Khramov, A.N.; Goncharov, G.I.; Komissarova, R.A.; Pisarevsky, S.A.; Pogarskaya, I.A.; Rzhevsky, Y.S.; Rodionov, V.P.; Slauzitais, I.P. *Paleomagnetology*; Nedra: Leningrad, Russia, 1982; 312p. (In Russian)

25. Kissel, C.; Laj, C. *Paleomagnetic Rotations and Continental Deformation*; NATO ASI Series: Mathematical and Physical Sciences; Kluwer Academic Publishers: Dordrecht, The Netherlands; Boston, MA, USA; London, UK, 1989; 530p.

26. Opdyke, N.D.; Channell, J.E.T. *Magnetic Stratigraphy*; International Geophysical Series; Academic Press: Cambridge, MA, USA, 1996; Volume 64, 361p.

27. Molostovsky, E.A.; Khramov, A.N. *Magnetostratigraphy and Its Importance in Geology*; Saratov University: Saratov, Russia, 1997; 172p. (In Russian)

28. Tauxe, L. *Paleomagnetic Principles and Practice*; Kluwer Academic Publishers: Dordrecht, The Netherlands; Boston, MA, USA; London, UK, 2003; 300p.

29. Sholpo, L.E. (Ed.) *The Use of Rock Magnetism in Geological Survey*; Nedra: Leningrad, Russia, 1986; 182p. (In Russian)

30. Ben-Avraham, Z.; Ginzburg, A.; Makris, J.; Eppelbaum, L. Crustal structure of the Levant basin, eastern Mediterranean. *Tectonophysics* **2002**, *346*, 23–43. [CrossRef]

31. Eppelbaum, L.V.; Nikolaev, A.V.; Katz, Y.I. Space location of the Kiama paleomagnetic hyperzone of inverse polarity in the crust of the eastern Mediterranean. *Dokl. Earth Sci.* **2014**, *457*, 710–714. [CrossRef]

32. Eppelbaum, L.V.; Katz, Y.I. Newly Developed Paleomagnetic Map of the Easternmost Mediterranean Unmasks Geodynamic History of this Region. *Cent. Eur. J. Geosci. Open Geosci.* **2015**, *7*, 95–117. [CrossRef]

33. Eppelbaum, L.V.; Katz, Y.I. Eastern Mediterranean: Combined geological-geophysical zonation and paleogeodynamics of the Mesozoic and Cenozoic structural-sedimentation stages. *Mar. Pet. Geol.* **2015**, *65*, 198–216. [CrossRef]

34. Eppelbaum, L.V.; Khesin, B.E. *Geophysical Studies in the Caucasus*; Springer: Berlin/Heidelberg, Germany; New York, NY, USA, 2012; 411p.

35. Irving, E.; Runcorn, S.K. Analysis of the palaeomagnetism of the Torridonian sandstone series of north-west Scotland. *Philos. Trans. R. Soc. Lond.* **1957**, *250*, 83–99.

36. Laj, C.; Channell, J.E.T. Geomagnetic Excursions. In *Geomagnetism*; Kono, M., Ed.; Series: Treatise on Geophysics; Elsevier: Amsterdam, The Netherlands, 2007; Volume 5, pp. 373–416.

37. Khramov, A.N. *Paleomagnetic Correlation of Sedimentary Strata*; Australian National University: Canberra, Australia, 1960; 204p.

38. Picard, M.D. Paleomagnetic correlation of units within Chugwater (Triassic) formation, west-central Wyoming. *Am. Assoc. Pet. Geol. Bull.* **1964**, *48*, 269–291.

39. Irving, E. Paleomagnetism of some Carboniferous rocks from New South Wales and its relation to geological events. *J. Geophys. Res.* **1966**, *71*, 6025–6051. [CrossRef]

40. Vine, F.J.; Matthews, D.H. Magnetic anomalies over ocean ridges. *Nature* **1963**, *199*, 947–949. [CrossRef]

41. Pitman, W.G., III; Larson, L.R.; Herron, E.M. *Age of Ocean Basalts Determined from Magnetic Anomaly Lineation*; Geological Society of America: Boulder, CO, USA, 1974.

42. Cande, S.C.; Kent, D.V. A new geomagnetic polarity time scale for the Late Cretaceous and Cenozoic. *J. Geophys. Res.* **1992**, *97*, 13917–13951. [CrossRef]

43. Shreyder, A.A. Chronology of linear marine magnetic anomalies. *Izv. Phys. Solid Earth* **1993**, *9*, 305–319.

44. Tominaga, M.; Sager, W.W.; Tivey, M.A.; Lee, S.-M. Deep-tow magnetic anomaly study of the Pacific Jurassic Quiet Zone and implications for the geomagnetic polarity reversal timescale and geomagnetic field behavior. *J. Geophys. Res.* **2008**, *113*, B07110. [CrossRef]

45. McDougall, I.; Saemundsson, K.; Johannesson, H.; Watkins, N.D.; Kristjansson, L. Extension of the geomagnetic polarity time scale to 6.5 m.y.: K-Ar dating, geological and paleomagnetic study of a 3,500-m lava succession in western Iceland. *Geol. Soc. Am. Bull.* **1977**, *88*, 1–15. [CrossRef]

46. Molostovsky, E.A. Paleomagnetic Method for Sedimentary Rock Mapping. In *Application of Rock Magnetism for Geological Mapping*; Nedra: Leningrad, Russia, 1986; pp. 158–166. (In Russian)

47. Glevasskaya, A.M.; Mikhailova, N.P. Paleomagnetic Mapping of Volcanogenic Rocks. In *Application of Rock Magnetism for Geological Mapping*; Nedra: Leningrad, Russia, 1986; pp. 166–176. (In Russian)

48. Kristjansson, L.; Jonsson, G. Paleomagnetism and magnetic anomalies in Iceland. *J. Geodyn.* **2007**, *43*, 30–54. [CrossRef]

49. Goguitchaichvili, A.; Cervantes, M.A.; Calvo-Rathert, M.; Camps, P.; Sologashvili, J.; Maissuradze, G. Gilbert-Gauss Geomagnetic Reversal Recorded in Pliocene Volcanic Sequences from Lesser Caucasus: Revisited. *Earth Planets Space* **2009**, *61*, 71–82. [CrossRef]

50. Nur, A.; Ron, H.; Scott, O. Mechanics of Distributed Fault and Block Rotation. In *Paleomagnetic Rotations and Continental Deformation*; NATO ASI Series: Mathematical and Physical Sciences; Kissel, C., Laj, C., Eds.; Kluwer Acad. Publishers: Dordrecht, The Netherlands; Boston, MA, USA; London, UK, 1989; pp. 209–228.

51. Granot, R.; Abelson, M.; Ron, H.; Agnon, A. The oceanic crust in 3D: Paleomagnetic reconstruction in the Troodos ophiolite gabbro. *Earth Planet. Sci. Lett.* **2006**, *251*, 280–292. [CrossRef]

52. Rolland, Y. Caucasus collisional history: Review of data from East Anatolia to West Iran. *Gondwana Res.* **2017**, *49*, 130–146. [CrossRef]

53. Eppelbaum, L.; Katz, Y. Significant tectono-geophysical features of the African-Arabian tectonic region: An overview. *Geotectonics* **2020**, *54*, 266–283. [CrossRef]

54. Gvirtzman, G.; Klang, A.; Rotstein, Y. Early Jurassic shield volcano below Mount Carmel: New interpretation of the magnetic and gravity anomalies and implication for Early Jurassic rifting. *Isr. J. Earth Sci.* **1990**, *39*, 149–159.

55. Ginzburg, A.; Eppelbaum, L. *A Combined 3D Interpretation of the Carmel Gravity and Magnetic Anomalies*; Oilfields Ltd.: Tel Aviv, Israel, 1993; pp. 1–42.

56. Eppelbaum, L.; Katz, Y.; Ben-Avraham, Z. Mt. Carmel structure as a plate tectonics phenomenon. In Proceedings of the Annual Conference of the Israel Geological Society, Beit-Shean, Israel, 19–21 February 2006; p. 31.

57. Segev, A.; Sass, E. *The Geology of the Carmel Region, Albian-Turonian Volcano-Sedimentary Cycles on the Northwestern Edge of the Arabian Platform*; Report of the Israel Geological Soc.; Israel Geological Society: Jerusalem, Israel, 2009; pp. 1–77.

58. Lu, J.-G.; Griffin, W.L.; Huang, J.-X.; Dai, H.-K.; Castillo-Oliver, M.; O'Reilly, S.Y. Structure and composition of the lithosphere Mount Carmel, North Israel. *Contrib. Mineral. Petrol.* **2022**, *177*, 1–29. [CrossRef]

59. Garfunkel, Z.; Almagor, G. Geology and structure of the continental margin off northern Israel and the adjacent part of the Levantine basin. *Mar. Geol.* **1985**, *62*, 105–131. [CrossRef]

60. Gvirtzman, G.; Steinitz, G. *The Asher Volcanics—An Early Jurassic Event in the Northern Israel*; Current Research; Geological Survey of Israel: Jerusalem, Israel, 1982; pp. 28–33.

61. Garfunkel, Z. Tectonic setting of Phanerozoic magmatism in Israel. *Israel J. Earth Sci.* **1989**, *38*, 51–74.

62. Garfunkel, Z.; Derin, B. Reevaluation of the latest Jurassic-Early Cretaceous history of the Negev and the role of magmatic activity. *Isr. J. Earth Sci.* **1988**, *37*, 43–52.

63. Dvorkin, A.; Kohn, B.P. The Asher volcanics, northern Israel: Petrography, mineralogy, and alteration. *Isr. J. Earth Sci.* **1989**, *38*, 105–123.

64. Kaminchik, J.; Segev, A.; Katzir, Y. The Origin of Intraplate Alkaline Mafic Magmatism in Continental Shelves: Lavas and Xenoliths from the Upper Cretaceous Volcanos of Mt. Carmel. Master's Thesis, Beer-Sheva University, Beersheba, Israel, 2014, *unpublished*.

65. Griffin, W.L.; Gain, S.E.M.; Huang, J.-X.; Belousova, E.A.; Toledo, V.; O'Reilly, S.Y. Permian to quaternary magmatism beneath the Mt Carmel area, Israel: Zircons from volcanic rocks and associated alluvial deposits. *Lithos* **2018**, *314–315*, 307–322. [CrossRef]

66. Esperanca, S.; Garfunkel, Z. Ultramafic xenoliths from the Mt. Carmel area (Karem Maharal volcano), Israel. *Lithos* **1986**, *19*, 43–49. [CrossRef]

67. Mittlefehldt, D.W. Petrology of high pressure clinopyroxenite series xenoliths, Mount Carmel, Israel. *Contrib. Mineral. Petrol.* **1986**, *94*, 245–252. [CrossRef]

68. Apter, D.B. High pressure indicator minerals from the Rakefet magmatic complex (RMC). Mt. Carmel, Israel. In Proceedings of the Geological Society of South Africa Kimberley Diamond Symposium, Kimberley, South Africa, 11–13 September 2014.

69. Dobrzhinetskaya, L.; Mukhin, P.; Wang, Q.; Wirth, R.; O'Bannon, E.; Zhao, W.; Eppelbaum, L.; Sokhonchuk, T. Moissanite (SiC) with metal-silicide and silicon inclusions from tuff of Israel: Raman spectroscopy and electron microscope studies. *Lithos* **2018**, *310–311*, 355–368. [CrossRef]

70. Nur, A.; Helsey, C.F. Palaeomagnetism of Tertiary and Recent lavas of Israel. *Earth Planet. Sci. Lett.* **1971**, *10*, 375–379. [CrossRef]

71. Lang, B.; Mimran, Y. An Early Cretaceous volcanic sequence in central Israel and its significance to the absolute date of the base of the Cretaceous. *J. Geol.* **1985**, *93*, 179–184. [CrossRef]

72. Lang, B.; Steinitz, G. K-Ar dating of Mesozoic magmatic rocks in Israel: A review. *Isr. J. Earth Sci.* **1989**, *38*, 89–103.

73. Shaliv, G. Stages in the Tectonics and Volcanic History of the Neogene Basin in the Lower Galilee and the Valleys. Ph.D. Thesis, Hebrew University of Jerusalem, Jerusalem, Israel, 1991. (In Hebrew, Summary in English)

74. Mor, D. A time-table for the Levant Volcanic Province, according to K-Ar dating in the Golan Heights, Israel. *J. Afr. Earth Sci.* **1993**, *16*, 223–234. [CrossRef]

75. Heimann, A.; Steinitz, G.; Mor, D.; Shaliv, G. The Cover Basalt Formation, its age and its regional and tectonic setting: Implications from K-Ar and ^{40}Ar/^{39}Ar geochronology. *Isr. J. Earth Sci.* **1996**, *45*, 55–71.

76. Sneh, A.; Bartov, Y.; Rozensaft, M. *Geological Map of Israel, Scale 1:200,000*; Geol. Survey of Israel; Ministry of National Infrastructure: Jerusalem, Israel, 1998.

77. Katz, Y.I.; Eppelbaum, L.V. Levantine phase of tectonic-thermal activity in the Eastern Mediterranean. *Trans. Annu. Meet. Geol. Soc. Am. Sect. Planet. Geol.* **1999**, *31*, A119.

78. Segev, A. Synchronous magmatic cycles during the fragmentation of Gondwana: Radiometric ages from the Levant and other provinces. *Tectonophysics* **2000**, *325*, 257–277. [CrossRef]

79. Segev, A. ^{40}Ar/^{39}Ar and K-Ar geochronology of Berriasian-Hauteririan and Cenomanian tectomagmatic events in northern Israel: Implications for regional stratigraphy. *Cretac. Res.* **2009**, *30*, 818–828. [CrossRef]

80. Segev, A.; Sass, E.; Ron, H.; Lang, B.; Kolodny, Y.; McWilliams, M. Stratigraphic, geochronologic, and paleomagnetic constraints on Late Cretaceous volcanism in northern Israel. *Isr. J. Earth Sci.* **2002**, *51*, 297–309. [CrossRef]

81. Ilani, S.; Harlavan, Y.; Tarawneh, K.; Rabba, I.; Weinberger, R.; Ibrahim, K.; Peltz, S.; Steinitz, G. New K-Ar ages of basalts from the Harrat Ash Shaam volcanic field in Jordan: Implications for the span and duration of the upper mantle upwelling beneath the western Arabian plate. *Geology* **2001**, *29*, 171–174. [CrossRef]

82. Ilani, S.; Kafri, U.; Harlavan, Y. Campanian volcanism within the Asher-1 borehole. *Isr. J. Earth Sci.* **2005**, *54*, 179–181. [CrossRef]

83. Karcz, J.; Sneh, A. *Sheet 3-I, Haifa. Geological Map of Israel, Scale 1:50,000*; Geological Survey of Israel: Jerusalem, Israel, 2011; Volume 50.

84. Sass, E.; Dekel, A.; Sneh, A. *Sheet 5-II, Umm el Fahm. Geological Map of Israel, Scale 1:50,000*; Geological Survey of Israel: Jerusalem, Israel, 2013.

85. Dembo, N.; Hamiel, Y.; Granot, R. *Intraplate Rotational Deformation Induced by Faults: Carmel-Gilboa Fault System as a Case Study*; Report No. GSI/19/2015; Geological Survey of Israel: Jerusalem, Israel, 2015; pp. 1–32.

86. Sneh, A. *Sheet 3-II, Shefar'Am. Geological Map of Israel, Scale 1: 50,000*; Geological Survey of Israel: Jerusalem, Israel, 2013.

87. Sneh, A. *Sheet 3-IV, Nazerat. Geological Map of Israel, Scale 1:50,000*; Geological Survey of Israel: Jerusalem, Israel, 2018.

88. Sneh, A.; Sass, E.; Bein, A.; Arad, A.; Rosensaft, M. *Sheet 5-I, Hadera. Geological Map of Israel, Scale 1:50,000*; Geological Survey of Israel: Jerusalem, Israel, 2014.

89. Fleischer, L.; Varshavsky, A. *A Lithostratigraphic Data Base of Oil and Gas Wells Drilled in Israel*; Rep. OG/9/02; Ministry of National Infrastructures of Israel: Jerusalem, Israel, 2012.

90. Segev, A.; Lang, B. 40Ar/39Ar dating of Valanginian top Tayasir Volcanics in the Mount Hermon area, northern Israel. Israel Geological Survey. *Curr. Res.* **2002**, *13*, 100–104.

91. Folkman, Y. Magnetic and Gravity Investigations of the Crustal Structure in Israel. Ph.D. Thesis, Tel Aviv University, Tel Aviv, Israel, 1976. (In Hebrew, English Abstract)

92. Eppelbaum, L.V.; Ben-Avraham, Z.; Katz, Y.; Cloetingh, S.; Kaban, M. Combined Multifactor Evidence of a Giant Lower-Mantle Ring Structure below the Eastern Mediterranean. *Positioning* **2020**, *11*, 11–32. [CrossRef]

93. Garfunkel, Z.; Zak, I.; Freund, R. Active faulting in the Dead Sea Rift. *Tectonophysics* **1981**, *80*, 1–26. [CrossRef]

94. Ben-Avraham, Z.; ten-Brink, U.; Bell, R.; Reznikov, M. Gravity field over the Sea of Galilee: Evidence for a composite basin along a transform fault. *J. Geophys. Res.* **1996**, *101*, 533–544. [CrossRef]

95. Ron, H.; Freund, R.; Garfunkel, Z.; Nur, A. Block rotation by strike-slip faulting: Structural and paleomagnetic evidence. *J. Geophys. Res.* **1984**, *89P*, 6256–6270. [CrossRef]

96. Heimann, A.; Ron, H. Geometric changes of plate boundaries along part of the Northern Dead Sea transform—Geochronological and paleomagnetic evidence. *Tectonics* **1993**, *12*, 477–491. [CrossRef]

97. Heimann, A. The Development of the Dead Sea Rift and Its Margins in Northern Israel during the Pliocene and Pleistocene. Ph.D. Thesis, Hebrew University of Jerusalem, Jerusalem, Israel, 1990. (In Hebrew, Summary in English)

98. Hurwitz, S.; Garfunkel, Z.; Ben-Gai, Y.; Reznikov, M.; Rotstein, Y.; Gvirtzman, H. The tectonic framework of a complex pull-apart basin: Seismic reflection observations in the Sea of Galilee, Dead Sea transform. *Tectonophysics* **2002**, *359*, 289–306. [CrossRef]

99. Heimann, A.; Braun, D. Quaternary stratigraphy of the Kinarot Basin, Dead Sea Transform, northeastern Israel. *Isr. J. Earth Sci.* **2000**, *49*, 31–44. [CrossRef]

100. Segev, A. *Zemah-1, A Unique Deep Oil Well on the Dead Sea Fault Zone, Northern Israel: A New Stratigraphic Amendment*; Report GSI/21/2017; Geological Survey of Israel: Jerusalem, Israel, 2017; pp. 1–27.

101. Frank, U.; Schwab, M.J.; Negendank, J.F.W. A lacustrine record of paleomagnetic secular variations from Birkat Ram, Golan Heights (Israel) for the last 4400 years. *Phys. Earth Planet. Inter.* **2002**, *133*, 21–34. [CrossRef]

102. Freund, R.; Oppenheim, M.J.; Schulman, N. Direction of magnetization of some basalts in the Jordan Valley and Lower Galilee (Israel). *Isr. J. Earth Sci.* **1965**, *14*, 37–74.

103. Behar, G.; Shaar, R.; Tauxe, L.; Asefaw, H.; Ebert, Y.; Heimann, A.; Koppers, A.A.P.; Ron, H. Paleomagnetism and paleosecular variations from the Plio-Pleistocene Golan Heights volcanic plateau, Israel. *Geochem. Geophys. Geosyst.* **2019**, *20*, 4319–4334. [CrossRef]

104. Rotstein, Y.; Bartov, Y. Seismic reflection across a continental transform: An example from a convergent segment of the Dead Sea rift. *J. Geophys. Res.* **1989**, *94*, 2902–2912. [CrossRef]

105. Heimann, A.; Steinitz, G. Fault systems in the south-western Hula Valley and the eastern slopes of the Galilee—Dating and tectonic implications. In Proceedings of the Israel Geological Society Meeting, Ramot, Israel, 2–5 April 1989; pp. 73–75.

106. Schattner, U.; Weinberger, R. A mid-Pleistocene deformation transition in the Hula basin, northern Israel: Implications for the tectonic evolution of the Dead Sea Fault. *Geochem. Geophys. Geosyst.* **2008**, *9*, 1–18. [CrossRef]

107. Mor, D.; Steinitz, G. *K-Ar Age of the Cover Basalts Surrounding the Sea of Galilee*; Rep. Me/6/82; Geological Survey of Israel: Jerusalem, Israel, 1982; 14p.

108. Shulman, H.; Reshev, M.; Ben-Avraham, Z. The structure of the Golan Heights and its tectonic linkage to the Dead Sea Transform and the Palniyrides folding. *Israel J. Earth Sci.* **2004**, *53*, 225–237. [CrossRef]

109. Meiler, M.; Reshef, M.; Shulman, H. Seismic depth-domain stratigraphic classification of the Golan Heights, central Dead Sea Fault. *Tectonophysics* **2011**, *510*, 354–369. [CrossRef]

110. Marcus, E.; Slager, J. The sedimentary-magmatic sequence of the Zemah-1 well (Jordan–Dead Sea Rift, Israel) and its emplacement in time and space. *Isr. J. Earth Sci.* **1985**, *34*, 1–10.

111. Eppelbaum, L.; Katz, Y. Tectonic-Geophysical Mapping of Israel and eastern Mediterranean: Implication for Hydrocarbon Prospecting. *Positioning* **2011**, *2*, 36–54. [CrossRef]

112. Kazmin, V.G. *Rift Structures of the Eastern Africa—The Split of the Continent and the Emergence of the Ocean*; Nauka: Moscow, Russia, 1987; 210p. (In Russian)